Mode-selecting effects and coherence in hot-plasma x-ray lasers

G. Hazak and A. Bar-Shalom
Nuclear Research Centre–Negev, P.O. Box 9001 Beer-Sheva, Israel
(Received 27 September 1988; revised manuscript received 30 May 1989)

The three-dimensional time-dependent set of Maxwell-Bloch equations for amplified spontaneous emission in diffraction-dominated (low Fresnel number) and small-gain systems is solved. The explicit form of the modes of radiation for gain and density profiles which are typical of hot-plasma x-ray-laser experiments is derived. The behavior of the excitation strengths of the modes is analyzed. It is found that due to the combined effects of diffraction, refraction, and gain, the excitation strength is a more rapidly decreasing function of the mode number in systems with smaller Fresnel numbers. The behavior of coherence as a function of propagation length in systems with various Fresnel numbers is computed and analyzed.

I. INTRODUCTION

In the past few years, several groups have reported success in getting amplified spontaneous emission (ASE) at soft-x-ray wavelengths out of hydrogenlike and neonlike ions in hot laboratory plasma.[1] The development of these amplifiers into bright sources of coherent radiation at wavelengths in the range of $\lambda = 22-44$ Å (the "water window") will open the road to the creation of holograms of live biological samples.[2,3]

The present experimental setups are capable (at least theoretically) of generating pulses of 1-MW radiation from plasma sources of length $L \cong 3$ cm and radius $R \cong 200$ μm.[3] Due to the large Fresnel number of these systems ($F = R^2/\lambda L \cong 66$) the number of spatial modes in the output radiation is large ($n \cong F^2 \cong 4000$), yielding low spatial coherence.

A method to obtain 1 MW of single-transverse-mode radiation was suggested by Rosen, Trebes, and Matthews.[3] Their method is based on driving the amplifier by single mode of radiation from a thin long preamplifier. The only requirement from the preamplifier intensity is that it be higher than the spontaneous noise in the main amplifier. In order to achieve single-transverse-mode radiation, the radius of the preamplifier must be of the order of 25 μm (corresponding to a Fresnel number of the order of 1). The subject of this work is to study the physical effects which lead to mode filtering in amplified spontaneous emission (ASE) in such small Fresnel number systems.

Previous treatments of radiation propagation in hot-plasma x-ray lasers were based on ray tracing.[4,5] London[4] has analyzed intensity amplification in the steady state of ASE by the radiative transfer method, namely, following ray trajectories and modeling the plasma by a medium with prescribed gain refractive index and density of radiating sources. In order to analyze problems such as transverse and longitudinal coherence the more refined semiclassical laser theory, which includes the wave behavior of the radiation as well as the dynamics of atomic polarization should be used. The progress in the last two decades in the theory of superfluorescence[6(a)] (SF) stimulated Raman scattering,[7] (SRS) and ASE,[6(b)] can help us in this task. It was shown that a complete quantum-mechanical description of SF, SRS, and ASE is given by a set of equations for the field and polarization operators which are formally identical to the set of Maxwell-Bloch equations of the semiclassical theory of laser-atom interaction, with an additional stochastic Langevin term. This theoretical framework can now be used and further developed, in order to analyze results such as transverse coherence and power spectrum obtained in x-ray laser (XRL) experiments. Such a program was initiated by us in Ref. 5. The model equations were solved, in the limit of large Fresnel numbers (negligibly small diffraction effects), by the ray-tracing technique, yielding formulas for the field intensity, field autocorrelation function, complex degree of coherence, and power spectrum. The results of Ref. 5 are useful in the analysis of the present XRL experiments,[1] which are mainly single-pass ASE experiments with large Fresnel numbers.

In the preamplifier proposed by Rosen, Trebes, and Matthews[3] one expects that, due to small Fresnel numbers, diffraction will play an essential role in determining the characteristics of the output radiation. For such systems the expansion in $1/F$, used in Ref. 5, which leads to a geometric-optics-like solution of the model equations is not valid and a complete treatment of the wave behavior of the radiation is required. The nature of the evolving field indicates also the appropriate mathematical approach to the solution. Due to the filtering effect, small-Fresnel-number systems support only a small number of modes. Elementary analysis of transverse coherence,[8] early works on optical resonators,[9] and more recent works on transverse coherence of SF (Ref. 10) and SRS [(Ref. 7(b)] all show that, in a system initiated with a random signal, the number of transverse coherent modes that survive at the end of the system is $n \sim 4\pi^2 R^4/\lambda^2 L^2 = F^2$. Obviously field evolution in small-Fresnel-number systems is best handled by expanding the field in a set of coherent fields (modes) with random coefficients. Such an analysis was successfully applied (to SRS) for a square gain profile.[7(b)] The functional shapes of the modes and their excitation strengths were found by using the known propagator of the wave equation in a homogeneous medium as a kernel of the integral equation for the modes. The integral equation was solved numerically. This method is limited to a square gain profile.

For the purpose of analyzing transverse coherence in XRL experiments gain profiles other than square have to be considered. In this work we present a method for evaluating the modes, their excitation strengths, and the coherence of the output radiation for a general gain profile. The method is simple and analytically solvable for the class of gain and density profiles of the form

$$f\{\mathbf{r}_T^2/[R^2(1+z^2/L^2)]\}/(1+z^2/L^2)\ ,$$

where $\mathbf{r}_T$ and z are the coordinates perpendicular and parallel (respectively) to the long dimension of the system (the lasing axis); R and L are the transverse dimension and length of the system, respectively.

The plan of the paper is as follows. In Sec. II we present a brief review of the model equations for hot-plasma x-ray lasers. In Sec. III we expand the radiation field in Gaussian-Laguerre functions which constitute a complete orthonormal set of transversely localized solutions of the wave equation in free space. This expansion reduces the model equations to a set of coupled-mode equations (i.e., a set of coupled stochastic differential equations for the projections of the field on the modes). The solution of the coupled-mode equations is derived at the end of the section. This solution is used in Sec. IV to derive a formula for the mode expansion of the complex degree of coherence of the output radiation. The explicit form of the complex degree of coherence for the class of gain profiles of the form

$$g=f_1\{\mathbf{r}_T^2/[R^2(1+z^2/L^2)]\}/(1+z^2/L^2)\ ,$$

is given in Sec. V. In that section we also derive a representation of the actual modes of the system as an expansion in the set of Gaussian-Laguerre functions. In Sec. VI a numerical study of the actual modes, the excitation strengths, and the coherence of the output radiation is presented. Summary and discussion are given in Sec. VII.

II. THE BASIC EQUATIONS

The spatial and temporal evolution of the radiation field in hot-plasma XRL is governed by the set of linearized Maxwell-Bloch equations[5] in the rotation-wave slowly varying envelope approximation:

$$i\frac{\partial\Omega(\boldsymbol{\rho},\eta,\tau)}{\partial\eta}+\nabla_\rho^2\Omega(\boldsymbol{\rho},\eta,\tau)/2F +[\omega_p^2(\boldsymbol{\rho},\eta)(L/2\omega c)]\Omega(\boldsymbol{\rho},\eta,\tau)=\alpha\Gamma[\mathcal{P}(\boldsymbol{\rho},\eta,\tau)]_{\rm av}\ , \tag{1}$$

$$i\frac{\partial\mathcal{P}(\boldsymbol{\rho},\eta,\tau)}{\partial\tau}=\Delta\mathcal{P}(\boldsymbol{\rho},\eta,\tau)-W(\boldsymbol{\rho},\eta)\Omega(\boldsymbol{\rho},\eta,\tau) -i\gamma\mathcal{P}(\boldsymbol{\rho},\eta,\tau)+\mathcal{R}(\boldsymbol{\rho},\eta,\tau)\ . \tag{2}$$

In these equations, $\eta=z/L$, $\boldsymbol{\rho}=\mathbf{r}_T/R$ and $\tau=\tau-z/c$. $\mathbf{r}_T$ is perpendicular to the lasing axis z, R and L are the transverse and longitudinal scale lengths typical of the system, Ω is the normalized envelope of the radiation field E, $\mathcal{P}$ is the normalized envelope of the atomic polarization $\mathbf{p}$, W is the population inversion, $\mathcal{R}$ is the random Langevin force, and α is a dimensionless normalization factor (the numerical value of which is of the order of the gain-length product). Also,

$$\mathbf{E}(\mathbf{r}_T,z,t)=\mathbf{E}_0(\mathbf{r}_T,z,t)e^{(i\omega/c)(z-ot)}\ , \tag{3}$$

$$\Omega=|\mathbf{d}||\mathbf{E}_0|/\hbar\ , \tag{4}$$

$$\mathbf{p}=\mathbf{d}\mathcal{P}e^{(i\omega/c)(z-ct)}\ , \tag{5}$$

and

$$\Delta=(\varepsilon_1-\varepsilon_2)/\hbar-\omega\ , \tag{6}$$

$$\alpha=(3/8\pi)\lambda^2An_iL/\Gamma\ , \tag{7}$$

$$\mathbf{d}=\langle u_1|e\mathbf{R}_{\rm d}|u_2\rangle\ , \tag{8}$$

$$\omega_p^2=4\pi n_e e^2/m\ , \tag{9}$$

and

$$1/F=L/[R^2(\omega/C)]\ .$$

n_e and n_i are the electron and ion densities. e and m are the electron charge and mass. u_1, u_2, ε_1, and ε_2 are the eigenvectors and eigenvalues of the atomic Hamiltonian in the absence of radiation. Δ is the detuning between the radiation frequency and the atomic transition frequency. $e\mathbf{R}_{\rm d}$ is the atomic dipole operator. A is the Einstein coefficient, $A=(\frac{4}{3})|\mathbf{d}|^2\omega^3/(\hbar c^3)$. Δ_D is the full width at half maximum (FWHM) of the detuning distribution $d(\Delta)$. Γ is the total linewidth due to both homogeneous and inhomogeneous broadening effects. The averaging process $[\ ]_{\rm av}$ is over detunings due to different Doppler shifts of atoms moving with different velocities relative to the laboratory system. The $\gamma\mathcal{P}$ and $\mathcal{R}$ terms in Eq. (2) are relaxation and fluctuation terms, respectively, due to homogeneous dephasing effects[11] (γ is the decay rate due to phase changing collisions plus the sum of radiative decay rates of upper and lower levels divided by 2). Fluctuations at different times and locations do not correlate; furthermore, it may be shown that[7(a)]

$$\langle\mathcal{R}(\boldsymbol{\rho},\eta,\tau)\mathcal{R}(\boldsymbol{\rho}',\eta',\tau')\rangle =\delta^2(\boldsymbol{\rho}-\boldsymbol{\rho}')\delta(\eta-\eta')\delta(\tau-\tau')2\Gamma/(n_iR^2L)\ . \tag{10}$$

Equations (2) and (10) define the *random Langevin force* $\mathcal{R}$.

At the end of Sec. V it will be shown that, in the limit of very small gain, this definition leads to the correct spontaneous-emission rate. Also, initially the atomic polarizations at different locations do not correlate, and the following relation holds;[7(a)]

$$\langle\mathcal{P}(\boldsymbol{\rho},\eta,\tau=0)\mathcal{P}(\boldsymbol{\rho}',\eta',\tau'=0)\rangle =\delta^2(\boldsymbol{\rho}-\boldsymbol{\rho}')\delta(\eta-\eta')/(n_iR^2L)\ . \tag{11}$$

As a first step towards the solution of Eqs. (1) and (2) we perform a Laplace transform with respect to the time variable τ and eliminate p, thus reducing Eqs. (1) and (2) to a single equation,

$$i\frac{\partial\Omega^L}{\partial\eta}+\nabla_\rho^2\Omega^L/2F+(L/2\omega c)\omega_p^2\Omega^L -i\alpha W\Omega^L[\Gamma/(\gamma+s+i\Delta)]_{\text{av}} =\alpha[\mathcal{P}(\boldsymbol{\rho},\eta,0)-i\mathcal{R}^L][\Gamma/(\gamma+s+i\Delta)]_{\text{av}}\ . \tag{12}$$

In general the averaging process [in Eq. (12)] introduces the inhomogeneous line broadening, namely,

$$[1/(\gamma+s+i\Delta)]_{\text{av}}\approx 1/(\Gamma+s)\ .\ .$$

It may be shown that the total linewidth Γ may be approximated by the sum of the homogeneous width and the width of the Doppler line profile, namely, $\Gamma\approx\gamma+\Delta_D$. [For Lorenzian line shape $d(\Delta)=(\Delta_D/\pi)/(\Delta_D^2+\Delta^2)$ these results are exact[12].]

We therefore rewrite Eq. (12) in the form

$$i\frac{\partial\Omega^L}{\partial\eta}+\nabla_\rho^2\Omega^L/2F+(L/2\omega c)\omega_p^2\Omega^L-i\alpha W\Omega^L\Gamma/(\Gamma+s) =\alpha[\mathcal{P}(\boldsymbol{\rho},\eta,0)-i\mathcal{R}^L][\Gamma/(\Gamma+s)]\ . \tag{12$'$}$$

In Eqs. (12) and (12′) the Laplace transform of a general quantity f is defined by

$$L_{(s,\tau)}(f)=f^L(\boldsymbol{\rho},\eta,s)=\int_0^\infty e^{-s\tau}f(\boldsymbol{\rho},\eta,\tau)d\tau\ , \tag{13}$$

$$L_{(s,\tau)}^{-1}(f^L)=f(\boldsymbol{\rho},\eta,\tau)=\int_{-i\infty+b}^{i\infty+b}e^{-s\tau}f^L(\boldsymbol{\rho},\eta,s)ds\ , \tag{14}$$

where b is chosen so that all the singular points of $f^L(\boldsymbol{\rho},\eta,s)$ are to the left of the integration contour in the complex s plane.

III. COUPLED-MODE EQUATION

In this section we will use Eq. (12′) to derive a set of coupled stochastic differential equations for the projections of the field envelope on a complete set of coherent modes. This will serve us in the analysis of the field coherence in Sec. IV. We expand the field in the form

$$\Omega(\boldsymbol{\rho},\eta,\tau)=\sum_{l',p'}a_{p'}^{l'}(\eta,\tau)U_{p'}^{l'}(\boldsymbol{\rho},\eta)\ , \tag{15}$$

or equivalently,

$$\Omega^L(\rho,\eta,s)=\sum_{l',p'}a_{p'}^{Ll'}(\eta,s)U_{p'}^{l'}(\boldsymbol{\rho},\eta)\ . \tag{16}$$

$U_{p'}^{l'}(\boldsymbol{\rho},\eta)$ are the Gaussian Laguerre functions[11] which constitute a complete orthonormal set of transversely localized solutions to the free space paraxial wave equation, i.e.,

$$i\frac{\partial U_{p'}^{l'}(\boldsymbol{\rho},\eta)}{\partial\eta}+\nabla_\rho^2\frac{U_{p'}^{l'}(\boldsymbol{\rho},\eta)}{2F}=0\ , \tag{17}$$

$$\int_0^\infty\rho\,d\rho\int_0^{2\pi}d\phi\ U_p^{*l}(\rho,\phi,\eta)U_{p'}^{l'}(\rho,\phi,\eta)=\delta(l,l')\delta(p,p')\ . \tag{18}$$

where $\rho=|\boldsymbol{\rho}|$, ϕ is the angle between $\boldsymbol{\rho}$ and the x axis. The coupled-mode equation is obtained by using the expansion (16) in Eq. (12′), multiplying by $U_p^{*l}(\rho,\phi,\eta)$ and integrating over $\rho\,d\rho\,d\phi$ [with the help of relations (17) and (18)]. Using a gain profile of the form $\alpha w=\alpha_0w_0f(\rho^2,\eta)$ and a density profile of the form $\omega_p^2=\omega_{p0}^2u(\rho^2,\eta)$, the result is (for details see Appendix)

$$i\frac{\partial a_p^{Ll}(\eta,s)}{\partial\eta}-i[\alpha_0w_0\Gamma/(s+\Gamma)]\sum_{p'}\{N_{pp'}^l(\eta)\exp[2i(p-p')\tan^{-1}(\eta)]/F\zeta^2\}a_{p'}^{Ll}(\eta,s) +(L/2\omega c)\omega_{p0}^2\sum_{p'}\{D_{pp'}^l(\eta)\exp[2i(p-p')\tan^{-1}(\eta)]/F\zeta^2\}a_{p'}^{Ll}(\eta,s)=[\Gamma/(s+\Gamma)][B_p^l(\eta)-iA_p^{Ll}(\eta,s)]\ . \tag{19}$$

In the last equation the terms in the curley brackets are the overlap integrals of the gain and of ω_p^2 with the modes. $B_p^l(\eta)$ and $A_p^{Ll}(\eta,s)$ are the projections (on the modes) of the random source terms $\mathcal{P}(\rho,\eta,\tau=0)$ and $\mathcal{R}^L(\rho,\eta,s)$, respectively, and $\zeta^2=2(1+\eta^2)/F$. $N_{pp'}$ and $D_{pp'}$ are defined explicitly in the Appendix.

A more compact form of Eq. (19) is obtained by changing to new variables,

$$\theta=\tan^{-1}(\eta+\eta_0)\ , \tag{20}$$

$$Y_p^{Ll}(\eta,s)\equiv\exp(-2ip\theta)a_p^{Ll}(\eta,s)\ , \tag{21}$$

and using a vector and matrix notation. For example, $(\mathbf{a}^l(\eta,s))_{\text{p}}$ [the p component of the vector $\mathbf{a}^l(\eta,s)]\equiv a_p^{Ll}(\eta,s)$, $(Y^l(\eta,s))_{\text{p}}$ [the p component of the vector $\mathbf{Y}^l(\eta,s)]\equiv\mathbf{Y}_p^{Ll}(\eta,s)$, and $(\underline{N}^l(\eta))_{\text{p,p}'}$ [the p,p' element of the matrix $\underline{N}^l(\eta)]\equiv N_{p,p'}^{Ll}(\eta)$.

Defining the matrices

$$(\underline{p})_{p,p'}\equiv\delta(p,p')p \tag{22}$$

and

$$\underline{T}^l(\eta,s+\Gamma)\equiv[(\alpha_0w_0/2)\Gamma/(s+\Gamma)]\underline{N}^l(\eta) +i(L/4\omega c)\omega_{p0}^2\underline{D}^l(\eta)-2i\underline{p}\ , \tag{23}$$

the coupled-mode equation (19) takes the form

$$i\partial\mathbf{Y}^l(\theta,s)/\partial\theta-i\underline{T}^l(\theta,s+\Gamma)\mathbf{Y}^l(\theta,s) =[F\zeta^2(\theta)/2]\exp(-2i\underline{p}\theta) \times[-i\,\mathbf{A}^{Ll}(\theta,s)+\mathbf{B}^l(\theta)]\Gamma/(s+\Gamma)\ . \tag{24}$$

The solution for the stochastic vector of mode amplitudes $\mathbf{a}^l$ may be formally written in terms of the Green's function of Eq. (24). Defining the matrix $\underline{G}_0^l$, which is the solution of the equation

$$i\frac{\partial \underline{G}_0^l(\theta,\theta',s+\Gamma)}{\partial\theta}-i\underline{T}^l(\theta,s+\Gamma)\underline{G}_0^l(\theta,\theta',s+\Gamma)=0\ , \quad (25)$$

with the condition

$$\underline{G}_0^l(\theta,\theta,s+\Gamma)=\underline{I}$$

(unit matrix), and the matrix $\underline{G}^l$,

$$\underline{G}^l=e^{2i\underline{p}\theta}[\underline{G}_0^l/(s+\Gamma)]e^{-2i\underline{p}\theta'}\ . \quad (26)$$

It may be easily shown [using Eqs. (21), (24), (25), and (26) and assuming $\mathbf{a}^l(\theta=\theta_0)=0$, $\mathcal{P}(\theta=\theta_0)=0$] that the solution for the stochastic vector of mode amplitudes is

$$\mathbf{a}^l(\theta,\tau)=(\Gamma F/2)\int_0^\tau d\tau'\int_{\theta_0}^\theta d\theta' e^{-\Gamma(\tau-\tau')}\underline{G}^l(\theta,\theta',\tau-\tau')\zeta^2(\theta')[-i\,\mathbf{A}^l(\theta',\tau')+\delta(\tau')\mathbf{B}^l(\theta')]$$

or

$$\mathbf{a}^l(\eta,\tau)=\Gamma\int_0^\tau d\tau'\int_0^\eta d\eta' e^{-\Gamma(\tau-\tau')}\underline{G}^l(\eta,\eta',\tau-\tau')\times[-i\,\mathbf{A}^l(\eta',\tau')+\delta(\tau')\mathbf{B}^l(\eta')]\ . \quad (27)$$

IV. THE COMPLEX DEGREE OF COHERENCE

The analysis of transverse coherence of the output radiation, in hot-plasma XRL, is carried out in the present work by studying the properties of the complex degree of coherence defined by[8,13]

$$\mu(\rho,\phi,\theta,\tau{:}\sigma,\Phi,\Theta,T)=\frac{C(\rho,\phi,\theta,\tau{:}\sigma,\Phi,\Theta,T)}{[\langle|\Omega(\rho,\phi,\theta,\tau)|^2\rangle\langle|\Omega(\sigma,\Phi,\Theta,T)|^2\rangle]^{1/2}}\ , \quad (28)$$

where C is the field envelope autocorrelation function

$$C(\rho,\phi,\theta,\tau{:}\sigma,\Phi,\Theta,T)=\langle\Omega(\rho,\phi,\theta,\tau)\Omega^*(\sigma,\Phi,\Theta,T)\rangle. \quad (29)$$

As is shown in Ref. 13, by a simple example, the norm of the complex degree of coherence $|\mu(\rho,\phi,\theta,\tau{:}\sigma,\phi,\theta,\tau)|$ is equal to the visibility of the interference pattern in a double-slit Young's interference experiment with the output radiation as the source and the slits located at ρ and σ. Maximum coherence corresponds to $|\mu|=1$; partial coherence corresponds to $|\mu|<1$.

It has been demonstrated by many authors that the analysis of coherence is made simpler by using the notion of coherent modes.[14,7(b)] The expansion used in Sec. III [Eqs. (15) and (16)] with the help of the correlation law of the Langevin force and initial polarization [Eqs. (10) and (11)] yields the following mode expansion of the field envelope autocorrelation function:

$$C(\rho,\phi,\theta,\tau{:}\sigma,\Phi,\Theta,T)=\sum_{l,p,p'}U_p^l(\rho,\phi,\theta)U_{p'}^{l'}(\rho,\Phi,\Theta)\langle a_p^l(\theta,\tau)a_{p'}^l(\Theta,T)\rangle\ , \quad (30)$$

where the correlation matrix of mode amplitudes,

$$\langle a_p^l(\theta,\tau)a_{p'}^l(\Theta,T)\rangle\equiv\underline{M}(\theta,\tau,\Theta,T)\ , \quad (31)$$

is given by

$$\underline{M}(\theta,\tau,\Theta,T)=[\alpha_0^2/(8R^2Ln_0)]F^2\Gamma^2\int_0^\tau d\tau'\int_{\theta_0}^\theta d\theta' e^{-\Gamma(\tau-\tau')-\Gamma(T-\tau')}[2\Gamma+\delta(\tau')]\times[\underline{G}^l(\theta,\theta',\tau-\tau')e^{2i\underline{p}\theta'}\underline{D}^l(\theta')e^{-2i\underline{p}\theta'}\underline{G}^{*l}(\Theta,\theta',T-\tau')]\ . \quad (32)$$

Relations (30)–(32) establish a procedure for evaluating the complex degree of coherence for any given system which is characterized by a known geometry and the (three-dimensional) gain and electron density profiles. Explicitly, the procedure comprises the following steps.

(a) Use Eqs. (A3) and (A6) to evaluate the gain overlap matrix $\underline{N}$ and electron density overlap matrix $\underline{D}$; use Eqs. (22) and (23) to construct the matrix $\underline{T}$.

(b) Solve Eq. (25) for $\underline{G}_0^l(\theta,\theta';s+\Gamma)$: use relation (26) and the inverse Laplace transform in order to obtain the Green's matrix $\underline{G}^l(\theta,\theta',\tau)$.

(c) The complex degree of coherence $\mu,(\rho,\phi,\theta,\tau{:}\sigma,\Phi,\Theta,T)$ is obtained by inserting the results in relation (32) and using Eqs. (28), (29), (30), and (31).

In this procedure steps (a) and (c) are simple and easy for numerical implementation; step (b) is a bit problematic. The difficulty stems from the fact that in order to perform the inverse Laplace transform one has to solve Eq. (25) (which comprises a set of ordinary differential equations in θ) separately for every value of the transform variable s. The original equation for $\underline{G}^l(\theta,\theta',\tau)$ in θ,τ space is an integro-differential equation.

The difficulty may be removed if one is satisfied in evaluating the complex degree of coherence at the steady state established at late times $\tau\gg\alpha_0 g_p L/\Gamma$ (for the source for this inequality see Appendix B in Ref. 5). In order to evaluate the complex degree of coherence, in this limit, only $\underline{G}^l(\theta,\theta',s=0)$ is needed. Namely, in this case the set of ordinary differential equations (25) for $\underline{G}^l$ needs to be solved only once; this may be easily done numerically.

In the present work we wanted to also study the mechanisms which affect the transient evolution of coherence. For this purpose we have chosen an example of a family of gain and density profiles for which Eq. (25) could be analytically solved and $\underline{G}^l(\theta,\theta',\tau)$ could be evaluated both in the steady state and during the transient. This example is presented and analyzed in Sec. V. An extensive study of the steady-state behavior of coherence for various types of profiles [which require numerical solution of Eq. (25)] is left for a planned future work.

V. AN ANALYTICAL SOLUTION FOR A FAMILY OF GAIN PROFILES

The analysis of the complex degree of coherence [Eq. (28)] requires knowledge of the explicit solution of the Green's-function equation $\underline{G}_0$ [Eq. (25)] for the gain profile under consideration. In this section we present such an explicit solution for the family of gain and density profiles which have the following dependence on the coordinates $\mathbf{r}_T$ and z:

$$W(\mathbf{r}_T,z)\alpha(\mathbf{r}_T,z) = w_0\alpha_0 f_1[\mathbf{r}_T^2/R_1^2(1+z^2/L^2)]/(1+z^2/L^2) , \quad (33)$$

$$n_i(\mathbf{r}_T,z)=n_0 u[\mathbf{r}_T^2/R_2^2(1+z^2/L^2)]/(1+z^2/L^2) , \quad (34)$$

$$n_e=Zn_i , \quad (35)$$

where Z is the degree of ionization and w_0,α_0,n_0,R_1,R_2 are constants. It may be shown that (see the Appendix) in this case the matrix $\underline{T}$ is independent of θ. Consequently, the solution of the Green's-function equation [Eq. (25)] is

$$\underline{G}_0(\theta,\theta',s)=e^{\underline{T}(s)(\theta-\theta')} = \exp(\{[(\alpha_0 w_0/2)\Gamma/(s)]\underline{N}^l + i(L/4\omega c)\omega_{p0}^2\underline{D}^l-2i\underline{p}\}(\theta-\theta')) . \quad (36)$$

Using relation (26), diagonalizing $\underline{T}$, and performing the Laplace transform with the help of the formula[15]

$$L_{(s,\tau)}(e^{a/s}/s)=I_0[(4a\tau)^{1/2}] , \quad (37)$$

where I_0 is the modified Bessel function of order zero, we get the following solution for the Green's function:

$$[\underline{G}(\theta,\theta',\tau-\tau')]_{p-p'} = \sum_m \exp(ip\theta')K_{p,m}^{-1}\exp[i\lambda_m(\theta-\theta')] \times I_0\{[2\alpha_0 w_0\Gamma g_m(\theta-\theta')(\tau-\tau')]^{1/2}\} \times K_{m,p'}\exp(-ip'\theta) . \quad (38)$$

In Eq. (38), $K_{i,j}$ are the elements of the matrix which diagonalize the matrix $\underline{T}_0=(L/4\omega c)\omega_{p0}^2\underline{D}^l(\eta)-2\underline{p}$ and λ_p is the pth eigenvalue of $\underline{T}_0$, i.e.,

$$\sum_{m,m'} K_{p,m}^{-1}(\underline{T}_0)_{m,m'}K_{m',p'}=\delta(p,p')\lambda_p . \quad (39)$$

g_m is the first-order correction to the mth eigenvalue of $\underline{T}$ due to the gain matrix $\underline{N}$,

$$g_p=\sum_{m,m'} K_{p,m}^{-1}N_{m,m'}K_{m',p} . \quad (39')$$

In diagonalizing the matrix $\underline{T}$ we have treated the gain matrix as a small perturbation on the matrix $\underline{T}_0$. This approximation is justified since in XRL experiments refraction and diffraction dominate over the gain,

$$(L/4\omega c)\omega_{p0}^2 \gg \Gamma(\alpha_0 w_0/2)$$

(see also Appendix A in Ref. 5).

At this point we have in hand all the information necessary for the evaluation of the field envelope autocorrelation function; we define a new set of modes and a density overlap matrix,

$$V_p^l(\rho,\phi,\theta)=\sum_{p'} K_{p,p'}^{-1}e^{-2ip'\theta}U_{p'}^l(\rho,\phi,\theta) , \quad (40)$$

$$O_{p,p'}(\theta)=\sum_{m,m'} K_{p,m}^{-1}(D_{m,m'})K_{m',p'} . \quad (41)$$

The final formula for evaluating the field envelope autocorrelation function is obtained by inserting the Green's function [Eq. (38)] in the formula for the correlation matrix of mode amplitudes [Eq. (32)] and then inserting the result in Eq. (30), with the help of definitions (40) and (41). The final result is

$$C(\rho,\phi,\theta,\tau{:}\sigma,\Phi,\Theta,T) = \sum_{l,p,p'} V_p^{*l}(\rho,\phi,\theta)V_{p'}^l(\rho,\Phi,\Theta)X_{p,p'}(\theta,\Theta,\tau,T) , \quad (42)$$

where the correlation matrix of the new mode amplitudes is

$$X_{p,p'}(\theta,\Theta,\tau,T)=[\alpha_0^2/(8R^2Ln_0)]F^2\Gamma^2\int_0^\tau d\tau'\int_{\theta_0}^{\theta} d\theta' e^{-\Gamma(\tau-\tau')-\Gamma(T-\tau')}[2\Gamma+\delta(\tau')]O_{p,p'}(\theta') , \times\exp[i\lambda_p(\theta-\theta')-i\lambda_{p'}(\Theta-\theta')]I_0\{[2\alpha_0 w_0\Gamma g_p(\theta-\theta')(\tau-\tau')]^{1/2}\}I_0 \times\{[2\alpha_0 w_0\Gamma g_{p'}(\Theta-\theta')(T-\tau')]^{1/2}\} . \quad (43)$$

From the last equation we see that the assumption made in Ref. 7(b) that the correlation matrix of mode amplitudes is a diagonal matrix holds true only for the case of a homogeneous medium where the overlap matrices and the Green's matrix $\underline{G}$ are diagonal.

The definition of the new modes [Eq. (40)] helped us to reduce the diagonal terms of the correlation matrix, χ_{pp}, to a form similar to the one-dimensional correlation function, as can be seen by comparing Eq. (43) in the present work with Eq. (34) (with $\rho=\rho'=0$) in Ref. 5. Furthermore, the numerical examples described in Sec. VI show that while 100 Gauss-Laguerre modes U_p^l are needed in order to describe the solution, only 15 new modes are necessary in order to converge to the final form of the complex degree of coherence. These two properties indicate that the set of V_p^l modes is a natural set for the description of a radiation propagation in the presence of refraction and gain. In the rest of the work we shall use the name "actual modes" for the new modes V_p^l and "free space modes" for the traditional Gauss-Laguerre modes U_p^l.

In the rest of the section we shall derive two interesting simplified limiting forms of the correlation matrix [Eq. (43)].

(a) *Very-small-gain limit.* In the limit of very small gain the solution should predict the correct spontaneous-emission rate:

$$I \equiv \frac{|\mathbf{E}|^2}{4\pi\hbar\omega} \approx n_0 A z \ ,$$

where A is the Einstein coefficient. Indeed, using relations (4), (7), (33), (34), and (43) and the definition of the Einstein coefficient [in the paragraph after Eq. (9)] and following the method of Sec. III A in Ref. 7(a) it may be shown that for $w_0 = 1 \theta \approx \eta = z/L$ and $2\alpha_0 g_p \theta \ll 1$ we get that the rate of photon emission (per unit area) into the p mode is

$$\begin{aligned} I_{pp} &= \frac{\hbar^2 \chi_{pp}(\theta,\theta,\tau,\tau)c}{d^2 4\pi\hbar\omega} \\ &\approx (\tfrac{3}{128})(\pi R^2/L^2) A n_0 z (1 + e^{-2\Gamma\tau}\{I_0[(2\alpha_0 w_0 \Gamma g_p \theta\tau)^{1/2}] - I_1[(2\alpha_0 w_0 \Gamma g_p \theta\tau)^{1/2}]\}) \\ &\approx (\tfrac{3}{128})(\pi R^2/L^2) A n_0 z \ . \end{aligned}$$

(b) *Steady-state limit.* For the case $\theta = \Theta$, $\tau = T$, in the steady-state limit ($\tau \to \infty$) the integration $d\tau'$ in Eq. (43) may be performed analytically (using Eq. 6.615 in Ref. 15). The result is

$$\begin{aligned} X_{p,p'}(\theta,\theta,\tau\to\infty^*) = [\alpha_0^2/(4R^2 L n_0)] F^2 \Gamma^2 \int_{\theta_0}^{\theta} d\theta' O_{p,p'}(\theta') \exp[i\lambda_p(\theta-\theta') - i\lambda_{p'}(\theta-\theta')] \\ \times \exp[+\alpha_0 w_0 (g_p + g_{p'})(\theta-\theta')/4] I_0[\alpha_0 w_0 (g_p g_{p'})^{1/2}(\theta-\theta')/2] \ . \end{aligned} \tag{44}$$

In the limit of high gain, $\alpha_0 w_0 (g_p, g_{p'})^{1/2}(\theta-\theta') \gg 1$, I_0 may be replaced by the asymptotic value $I_0(x) \cong e^x/x^{1/2}$ and the correlation matrix of mode amplitudes takes the form

$$X_{p,p'}(\theta,\theta,\tau\to\infty^*) = [\alpha_0^2/(4R^2 L n_0)] F^2 \Gamma^2 \int_{\theta_0}^{\theta} d\theta' O_{p,p'}(\theta') \exp(\{+\alpha_0 w_0 [(g_p)^{1/2} + (g_{p'})^{1/2}]^2/4 + i\lambda_p - i\lambda_{p'}\}(\theta-\theta')) \ . \tag{45}$$

This last equation shows that g_p plays the role of the excitation strength of the mode V_p^l. In Sec. VI we shall use this explicit solution of the field envelope autocorrelation function for the detailed analysis of output radiation coherence.

VI. NUMERICAL ANALYSIS

In this section we study the coherence of systems with a gain profile of the family defined by relation (33). In order to be specific we will consider here the case

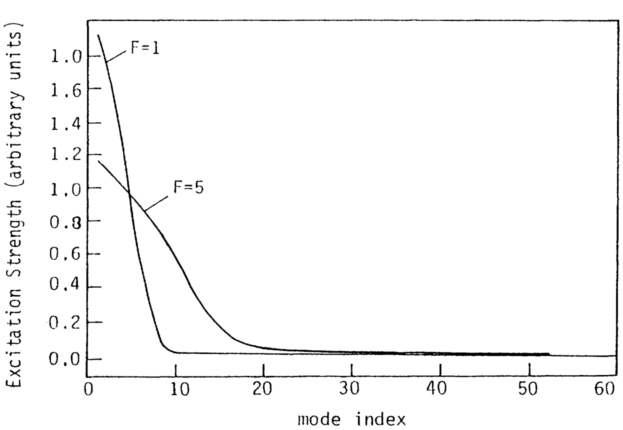

FIG. 1. Excitation strengths of the actual modes of the system as a function of mode index for $F = 1$ and 5.

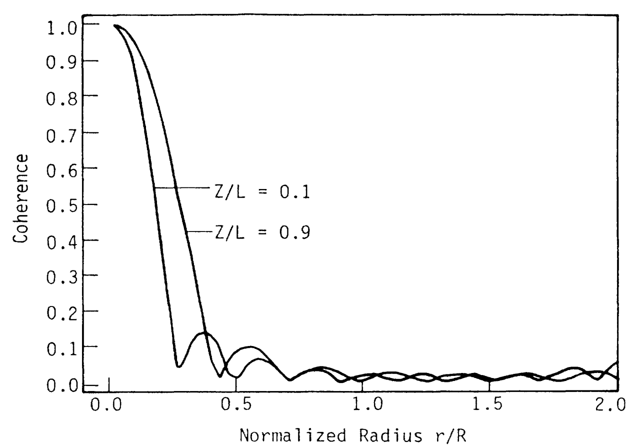

FIG. 2. Norm of the complex degree of coherence $|\mu(\rho,\phi=0,\theta,\tau\to\infty:\sigma=0,\phi=0,\theta,\tau\to\infty)|$ as a function of ρ for $\theta = 0.1$ and 0.733 (corresponding to $\eta = 0.1$ and 0.9) in a system with Fresnel number $F = 1$.

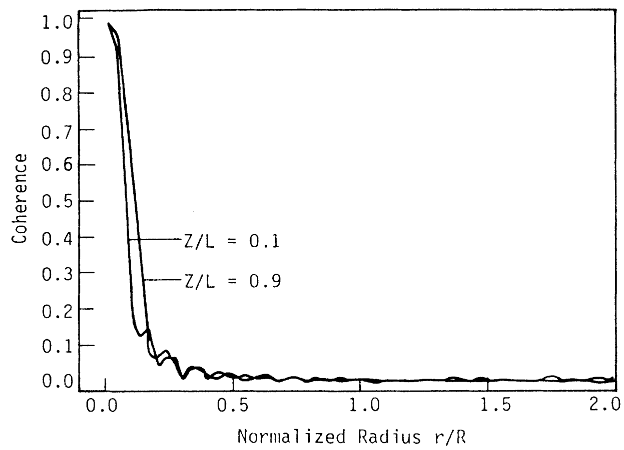

FIG. 3. Norm of the complex degree of coherence $|\mu(\rho,\phi=0,\theta,\tau\to\infty:\sigma=0,\phi=0,\theta,\tau\to\infty)|$ as a function of ρ for $\theta=0.1$ and 0.733 (corresponding to $\eta=0.1$ and 0.9) in a system with Fresnel number $F=5$.

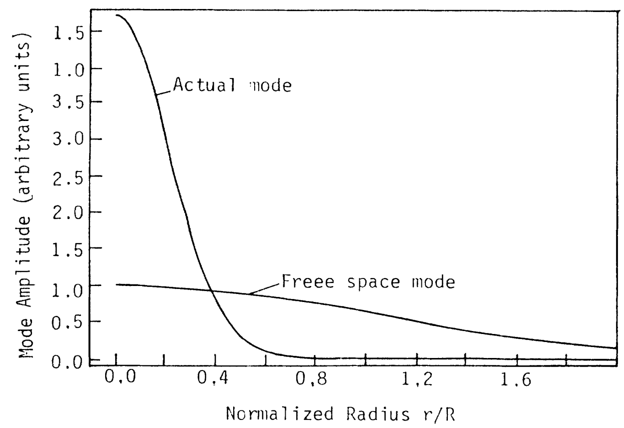

FIG. 4. First free space mode and first actual mode as a function of the normalized radius ρ ($F=1$).

$$W(\mathbf{r}_T,z)\alpha(\mathbf{r}_T,z) = w_0\alpha_0\exp[-\mathbf{r}_T^2/R_1^2(1+z^2/L^2)]/(1+z^2/L^2)\ , \tag{46}$$

$$n_i(\mathbf{r}_T,z)=n_0\exp[-\mathbf{r}_T^2/R_2^2(1+z^2/L^2)]/(1+z^2/L^2) \tag{47}$$

(with a gain-length product of $w_0\alpha_0=5$ and an ion density of $n_0=2\times10^{19}\ \mathrm{cm}^{-3}$; these numbers are representative of x-ray lasers[1]). For this gain and density profiles, the overlap matrices are analytically evaluated by the method of Ref. 16 and the Appendix. The matrix $\underline{N}$ takes the form

$$N_{p,p'}^{l}(\alpha)=\alpha^{l}\left[\frac{p!p'!}{(p+l)!(p'+l)!}\right]^{1/2}\sum_{m=0}^{p}\begin{bmatrix}p+l\\ m\end{bmatrix}\begin{bmatrix}p'+l\\ m+p-p'\end{bmatrix}\frac{(p-m+l)!}{(p-m)!}\alpha^{2(p-m)}(1-\alpha)^{2m+p-p'},\quad p>p' \tag{48}$$

where

$$\alpha=F/(F+1)\ . \tag{49}$$

Examination of the definition of the complex degree of coherence [Eqs. (28) and (29)] together with the explicit solution for the correlation function [Eqs. (42)–(45)] shows that the excitation strength $\{g_i\}$ (*defined as the real part of the eigenvalues of the matrix* $\underline{T}$) plays an essential role in determining the coherence of the output radiation. When the $\{g_i\}$ is a strongly peaked function of the eigenvalue indices p,l, only a few modes contribute to the sum in Eq. (42); the norm of the complex degree of coherence $|\mu(\rho,\phi,\theta,\tau:\sigma,\phi,\theta,\tau)|$ is closer to unity and consequently the output radiation is more coherent. In Fig. 1 the excitation strength of the modes is shown as a function of the mode index for two cases: Fresnel number$=1$ and Fresnel number$=5$. Clearly the decrease in excitation strength is much stronger for $F=1$, leading to a better transverse coherence in this case. In Figs. 2 and 3 we show the norm of the complex degree of coherence $|\mu(\rho,\phi=0,\theta,\tau\to\infty:\sigma=0,\phi=0,\theta,\tau\to\infty)|$ as a function of ρ for $\theta=0.1$ and 0.733 (corresponding to $\eta=0.1$ and 0.9). From these figures we see that, as expected, coherence is better for longer propagation length and larger Fresnel numbers. In Figs. 4 and 5 the first and third modes are plotted as a function of the normalized radius ρ. For comparison we also show the free space modes. From this figure we see that the actual modes of the system are more concentrated in the high-density regime than the corresponding free space modes.

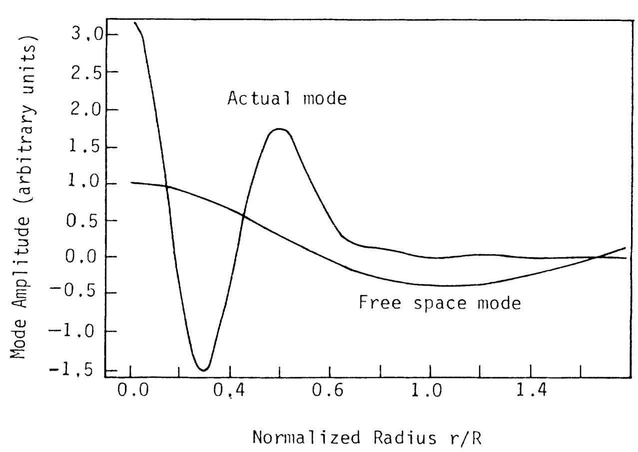

FIG. 5. Third free space mode and third actual mode as a function of the normalized radius ρ ($F=1$).

VII. SUMMARY AND DISCUSSION

The temporal and spatial evolution of a small signal radiation field in hot-plasma XRL is governed by the set of Maxwell-Bloch equations. [Eqs. (1) and (2) in the text.] The nature of the radiation field is determined by the Fresnel number of the system. The case of a large Fresnel number was treated in Ref. 5. It was shown that, correct to the lowest significant order of the expansion in the small parameter $1/F$, Maxwell-Bloch equations may be reduced to a set of equations which describe the evolution of the field characteristics (phase, amplitude, gain) along ray trajectories. The essence of the large-Fresnel-number approximation is in the transverse Laplacian term in the wave equation [Eq. (12) in the present work]. One represents the field envelope in a phase amplitude form and neglects a term of the form $(1/F^2)\nabla_\rho^2|\Omega|$ (which is responsible for diffraction) while keeping the terms

$$(1/F)\nabla_\rho[\ln(\Omega/|\Omega|)]\cdot\nabla_\rho|\Omega|,\quad (1/F)\nabla_\rho^2\ln(\Omega/|\Omega|)\ .$$

These terms together with the terms proportional to the square of the plasma frequency ω_p^2 and the population inversion W are responsible for refraction and gain and yield the ray equations. The final result is a prescription for evaluating objects such as the field intensity and coherence as a function of time and location in terms of the solution of coupled ray equations. This may serve as a tool for the analysis of the interplay between gain and refraction and their influence on the characteristics of the output radiation in existing x-ray laser experiments[1] which are large-Fresnel-number experiments.

In order to achieve a better transverse coherence, future experiments are planned with small Fresnel numbers.[3] In such systems diffraction is a major effect which determines field evolution, the $1/F$ expansion is not justified and the method developed in Ref. 5 is not applicable. The purpose of the present work was to derive a method (complimentary to the one developed in Ref. 5) to solve and analyze the Maxwell-Bloch equations for diffraction-dominated (small-Fresnel-number) systems. The method takes advantage of the fact that, due to diffraction, small-Fresnel-number systems can support only a few natural modes of radiation. Explicitly, the approximations applied in deriving the method are the following. (a) The coupled mode equation [Eq. (19) or equivalently Eq. (24)] is in fact an infinite set of coupled stochastic differential equations for the projections of the field envelope on a complete set of coherent modes. The solution involves a truncation. We have found that for Fresnel numbers ranging from 1 to 5 convergence in the spectrum of the matrix $\underline{T}$ and in the shape of the actual system modes [see Eq. (40)] was obtained for matrices of order 100×100. For larger Fresnel numbers larger matrices were necessary and the method becomes less practical. (b) In diagonalizing the matrix $\underline{T}$ [see Eqs. (39) and (39′)] we have treated the gain matrix as a small perturbation on the refraction-diffraction matrix $\underline{T}_0$. Indeed, in x-ray laser experiments refraction dominates over the gain (see Appendix A of Ref. 5 for details). (c) For small Fresnel numbers the real part of the spectrum of $\underline{T}$ (the excitation strengths) is a rapidly decreasing function of the mode index (see Fig. 1) and the elements of the correlation matrix of the amplitudes of the actual modes depend exponentially on the corresponding excitation strength [see Eqs. (43)–45)]. This indicates that only a few (much less than 100) elements and actual modes should be applied in evaluating the intensity and coherence. We have found for Fresnel numbers of 1–5, convergence (up to 1%) is already obtained for 15 modes.

As in the complementary method for large Fresnel numbers,[5] the final result in this work is a prescription for evaluating objects such as the field intensity and coherence as a function of time and space. This can serve as a tool for analyzing the role of diffraction, refraction, and gain in determining the characteristics of the output radiation field in various configurations of small-Fresnel-number systems.

Some multiple pass hot-plasma x-ray laser experiments have already been performed, using multilayer mirrors. In such experiments, in addition to improved amplification, also some improvement in the longitudinal coherence is expected. It is possible to generalize the theory of the present work and to include also mirrors and axial modes. This may be done by using the axial-transverse modes $U_{pq}^l=U_p^l\exp(2\pi iqc\tau/L)$ instead of the transverse modes U_p^l in the expansion. Relations (28) and (29) are of course useful also for the analysis of longitudinal coherence. We are at present developing a study along this line.

The linear theory presented here (and also in Ref. 5) is valid for systems with small gain-length product where the depletion of population due to induced emission is not significant (nonsaturated systems). This is the case in most existing hot-plasma x-ray laser experiments. Future experiments with longer lasing plasmas (and possibly higher gains) may approach saturation. The competition between modes near saturation may be estimated from the spatial overlapping the modes obtained from our linear theory [Eq. (40) in the text and Figs. 4 and 5]. The area of population inversion shared by different modes is a measure of mode competition. Of course, a more detailed study of the dynamics of mode competition in the saturated case requires a nonlinear theory which is out of the scope of the present work.

APPENDIX

The explicit form of the Gaussian Laguerre functions is [see Chap. (16) in Ref. 12]

$$U_p^l(\rho,\phi,\eta)=[2p!/\pi(p+l)!]^{1/2}(2^{1/2}\rho/\zeta)^l L_p^l(2\rho^2/\zeta^2)/\zeta\exp\{-\rho^2/\zeta^2-i[l\phi+F\rho^2/2b-(2p+l+1)\tan^{-1}\eta]\}\ , \tag{A1}$$

where $\rho=|\boldsymbol{\rho}|$, ϕ is the angle between $\boldsymbol{\rho}$ and the x axis, $\zeta=2(1+\eta^2)/F$ and $b=(\eta+1/\eta)$. The coupled-mode equation (19) is obtained by using the expansion (16) in Eq. (12) multiplying by $U_p^{*l}(\rho,\phi,\eta)$, integrating $\rho\,d\rho\,d\phi$ [with the help of relations (17) and (18)]. We use a gain of the form $\alpha(\rho,\eta)W(\rho,\eta)=\alpha_0 w_0 f(\rho^2,\eta)$. The coefficients of the resultant equations are

$$\begin{aligned}\alpha_0 w_0 \int_0^\infty \rho\, d\rho \int_0^{2\pi} d\phi\, U_p^{*l}(\rho,\phi,\eta) f(\rho^2,\eta) U_{p'}^{l'}(\rho,\phi,\eta) &= \delta(l,l')\alpha_0 w_0 \Big[\exp[2i(p-p')]\tan^{-1}(\eta/F\xi^2)[2p!/(p+l)!]^{1/2}[2p'!/(p'+l)!]^{1/2}F \\ &\quad \times \int_0^\infty \xi^2\beta\, dx\, L_p^l(\beta x) f(\xi^2\beta x,\eta) L_{p'}^l(\beta x)(\beta x)^l e^{-\beta x}/4\Big] \\ &\equiv \delta(l,l')\alpha_0 w_0 (N_{pp'}^{l'}(\eta)\{\exp[2i(p-p')\tan^{-1}(\eta)]\}/F\xi^2)=0 ,\end{aligned} \tag{A2}$$

where

$$\begin{aligned} N_{pp'}^{l'}(\eta) &= [2p!/(p+l)!]^{1/2}[2p'!/(p'+l)!]^{1/2}F \\ &\quad \times \int \xi^2\beta\, dx\, L_p^l(\beta x) f(\xi^2\beta x,\eta) L_{p'}^l(\beta x)(\beta x)^l \\ &\quad \times e^{-\beta x}/4 ,\end{aligned} \tag{A3}$$

$$\beta = F/(1+F) ,$$

and

$$x = 2\rho^2/\beta\xi^2 .$$

In the case where the gain profile is of the form

$$\begin{aligned}\alpha(\rho,\eta)W(\rho,\eta) &= \alpha_0 w_0 f(\rho^2,\eta) \\ &= \alpha_0 w_0 f_1(\rho^2/(1+\eta^2))/(1+\eta^2) ,\end{aligned}$$

we have

$$\begin{aligned} N_{pp'}^{l'} &= [2p!/(p+l)!]^{1/2}[2p'!/(p'+l)!]^{1/2} \\ &\quad \times \int \beta\, dx\, L_p^l(\beta x) f_1(\beta x/F) L_{p'}^l(\beta x)(\beta x)^l e^{-\beta x}/2 ,\end{aligned} \tag{A4}$$

namely, in this special case $N_{pp'}^{l'}$ is independent of η.

In the same way for density profile of the form

$$n_i(\rho^2,\eta) = n_0 u(\rho^2,\eta) ,$$

$$n_e(\rho^2,\eta) = Z n_0 u(\rho^2,\eta) ,$$

(Z is the ionization degree), or

$$\omega_p^2(\rho,\eta) = \omega_{p0}^2 u(\rho^2,\eta) ,$$

$$\alpha(\rho,\eta) = \alpha_0 u(\rho^2,\eta) ,$$

we have

$$\begin{aligned}\int_0^\infty \rho\, d\rho \int_0^{2\pi} d\phi\, U_p^{*l}(\rho,\phi,\eta) u(\rho^2,\eta) U_{p'}^{l'}(\rho,\phi,\eta) &= \delta(l,l')\Big[\exp[2i(p-p')\tan^{-1}(\eta/F\xi^2)][2p!/(p+l)!]^{1/2}[2p'!/(p'+l)!]^{1/2}F \\ &\quad \times \int \xi^2\beta\, dx\, L_p^l(\beta x) u(\xi^2\beta x,\eta) L_{p'}^l(\beta x)(\beta x)^l e^{-\beta x}/4\Big] \\ &\equiv \delta(l,l')\{D_{pp'}^{l'}(\eta)\{\exp[2i(p-p')\tan^{-1}(\eta)]\}/F\xi^2\} ,\end{aligned} \tag{A5}$$

where

$$\begin{aligned} D_{pp'}^{l'}(\eta) &= [2p!/(p+l)!]^{1/2}[2p'!/(p'+l)!]^{1/2}F \\ &\quad \times \int \xi^2\alpha\, dx\, L_p^l(\alpha x) u(\xi^2\alpha x,\eta) L_{p'}^l(\alpha x)(\beta x)^l \\ &\quad \times e^{-\beta x}/4 .\end{aligned} \tag{A6}$$

In the case where the density profile is of the form

$$u(\rho^2,\eta) = u_1(\rho^2/(1+\eta^2))/(1+\eta^2) ,$$

we have

$$\begin{aligned} D_{pp'}^{l'} &= [2p!/(p-l)!]^{1/2}[2p'!/(p'+l)!]^{1/2} \\ &\quad \times \int \beta\, dx\, L_p^l(\beta x) u_1(\beta x/F) L_{p'}^l(\beta x) \beta x)^l e^{-\beta x}/2 .\end{aligned} \tag{A7}$$

Again, in this special case $D_{pp'}^{l'}$ is independent of η. The projections of the random source terms on the right-hand side of Eq. (12) are

$$\begin{aligned} A_p^{Ll}(\eta,s) &= \int_0^\infty \rho\, d\rho \int_0^{2\pi} d\phi\, U_p^{*l}(\rho,\phi,\eta) \mathcal{R}^L(\rho,\phi,\eta,s)\alpha(\rho,\eta) ,\end{aligned} \tag{A8}$$

$$B_p^l(\eta) = \int_0^\infty \rho\, d\rho \int_0^{2\pi} d\phi\, U_p^{*l}(\rho,\phi,\eta) \mathcal{P}(\rho,\phi,\eta,s)\alpha(\rho,\eta) . \tag{A9}$$

[1]D. L. Matthews *et al.*, Phys. Rev. Lett. **54**, 110 (1985); T. N. Lee, *et al.*, *ibid.* **59**, 1185 (1987); B. J. MacGowan *et al.*, J. Appl. Phys. **61**, 5243 (1987); Phys. Rev. Lett. **59**, 2157 (1987); S. Suckewer *et al.*, *ibid.* **55**, 1753 (1985); G. Jamelot *et al.*, J. Phys. B **18**, 4647 (1985); J. P. Seely *et al.*, Opt. Commun. **54**, 289 (1985); C. Chenais-Popovics *et al.*, Phys. Rev. Lett. **59**, 2161 (1987).

[2]M. D. Rosen, R. A. London, and P. L. Hagelstein, Phys. Fluids **31**, 666 (1988).

[3]M. D. Rosen, J. E. Trebes, and D. L. Matthews, Comments Plasma Phys. Controlled Fusion **10**, 245 (1987).

[4]Richard A. London, Phys. Fluids **31**, 184 (1988).

[5]G. Hazak and A. Bar-Shalom, Phys. Rev. A **38**, 1300 (1988).

[6](a) See, for example, M. Gross and S. Haroche, Phys. Rep. **93**, 301 (1982), and the list presented in Refs. 11 and 12 of Ref. 7(a); (b) Frederic A. Hopf and Pierre Meystre, Phys. Rev. A **12**, 2534 (1975); F. Hopf, P. Meystre, and D. W. McLaughlin, *ibid.* **13**, 777 (1976).

[7](a) M. G. Raymer and J. Mostowski, Phys. Rev. A **24**, 1980 (1981); (b) M. G. Raymer, I. A. Walmsky, J. Mostowsky, and B. Sobolewska, *ibid.* **30**, 610 (1984).

[8]M. Born and E. Wolf, *Principles of Optics,* 4th ed. (Pergamon, New York, 1970).

[9]A. G. Fox and T. Li, Bell Syst. Tech. J. **40**, 453 (1961).

[10]P. D. Drummond and J. H. Eberly, Phys. Rev. A **25**, 3446 (1982).

[11]A. E. Seigman, *Lasers* (University Science Books, Mill Valley, CA, 1986).

[12]M. F. H. Schuurmans, Opt. Commun. **34**, 185 (1980).

[13]Jan Perina *Coherence of Light,* 2nd ed. (Reidel, Dordrecht, 1985).

[14]E. Wolf and G. S. Agarwal, J. Opt. Soc. Am. A **1**, 541 (1984).

[15]*Table of Integrals, Series, and Products,* edited by I. S. Gradshteyn and I. M. Ryzhik (Academic, New York, 1965).

[16]B. N. Perry, P. Rabiniwitz, and M. Newstein, Phys. Rev. A **27**, 1989 (1983).